



<http://www.diva-portal.org>

This is the published version of a paper published in *Geophysical Research Letters*.

Citation for the original published paper (version of record):

Fu, H., Cao, J., Khotyaintsev, Y., Sitnov, M., Runov, A. et al. (2013)

Dipolarization fronts as a consequence of transient reconnection: In situ evidence.

Geophysical Research Letters, 40(23): 6023-6027

<http://dx.doi.org/10.1002/2013GL058620>

Access to the published version may require subscription.

N.B. When citing this work, cite the original published paper.

Permanent link to this version:

<http://urn.kb.se/resolve?urn=urn:nbn:se:umu:diva-85795>

Dipolarization fronts as a consequence of transient reconnection: In situ evidence

H. S. Fu,^{1,2} J. B. Cao,¹ Yu. V. Khotyaintsev,² M. I. Sitnov,³ A. Runov,⁴ S. Y. Fu,⁵ M. Hamrin,⁶ M. André,² A. Retinò,⁷ Y. D. Ma,¹ H. Y. Lu,¹ X. H. Wei,⁸ and S. Y. Huang⁹

Received 5 November 2013; revised 25 November 2013; accepted 25 November 2013; published 10 December 2013.

[1] Dipolarization fronts (DFs) are frequently detected in the Earth’s magnetotail from $X_{\text{GSM}} = -30 R_E$ to $X_{\text{GSM}} = -7 R_E$. How these DFs are formed is still poorly understood. Three possible mechanisms have been suggested in previous simulations: (1) jet braking, (2) transient reconnection, and (3) spontaneous formation. Among these three mechanisms, the first has been verified by using spacecraft observation, while the second and third have not. In this study, we show Cluster observation of DFs inside reconnection diffusion region. This observation provides in situ evidence of the second mechanism: Transient reconnection can produce DFs. We suggest that the DFs detected in the near-Earth region ($X_{\text{GSM}} > -10 R_E$) are primarily attributed to jet braking, while the DFs detected in the mid- or far-tail region ($X_{\text{GSM}} < -15 R_E$) are primarily attributed to transient reconnection or spontaneous formation. In the jet-braking mechanism, the high-speed flow “pushes” the preexisting plasmas to produce the DF so that there is causality between high-speed flow and DF. In the transient-reconnection mechanism, there is no causality between high-speed flow and DF, because the frozen-in condition is violated. **Citation:** Fu, H. S., et al. (2013), Dipolarization fronts as a consequence of transient reconnection: In situ evidence, *Geophys. Res. Lett.*, 40, 6023–6027, doi:10.1002/2013GL058620.

1. Introduction

[2] Dipolarization fronts (DFs) [Nakamura et al., 2002; Runov et al., 2009] are kinetic boundaries [Sergeev et al., 2009; Fu et al., 2012a] embedded inside high-speed plasma flows. They have been detected in the Earth’s magnetotail from $X_{\text{GSM}} = -30 R_E$ to $X_{\text{GSM}} = -7 R_E$ in geocentric solar magnetospheric (GSM) coordinates [Schmid et al., 2011; Fu et al., 2012b; Liu et al., 2013], and they play key roles in transporting

energy fluxes [Volwerk et al., 2008; Nakamura et al., 2011; Hamrin et al., 2013], accelerating electrons [Khotyaintsev et al., 2011; Fu et al., 2011; Vaivads et al., 2011; Artemyev et al., 2012a; Zhou et al., 2013; Wu et al., 2013], and ions [Artemyev et al., 2012b; 2013; Birn et al., 2012] during substorm activity.

[3] It is still poorly understood at present how DFs are formed. Jet braking [Birn et al., 2011], transient reconnection [Sitnov et al., 2009; Sitnov and Swisdak, 2011], and spontaneous formation [Sitnov et al., 2013] have been suggested as possible mechanisms in simulations. Jet braking occurs primarily in the near-Earth magnetotail ($X_{\text{GSM}} > -10 R_E$). The DFs produced by this mechanism propagate tailward or along the azimuthal direction [Birn et al., 2011; Nakamura et al., 2011]. Due to the strong interaction between the high-speed flow and the preexisting plasma, ballooning/interchange instability [e.g., Pritchett and Coroniti, 2010; Lu et al., 2013] is frequently reported at DFs in this scenario. Transient reconnection, triggered by the external perturbation [Sitnov et al., 2009; Pritchett, 2010; Sitnov and Swisdak, 2011], changes the topology of magnetic field and then produces the DFs. In this scenario, DFs are formed in the ion diffusion region but then propagate outward. The spontaneous formation of DFs requires an accumulation of magnetic flux at the tailward end of a 2-D current sheet [Sitnov et al., 2013]. This accumulation of magnetic flux, seen as a hump in B_z^{GSM} , leads to the ion tearing instability, which then produces the DFs. The last two mechanisms are quite similar except that one (transient reconnection) involves X line and reconnection, while the other (spontaneous formation) does not need an X line.

[4] There have been observational evidences of the first mechanism (jet braking). The DFs formed via this mechanism are usually detected in the near-Earth region together with the rebound of high-speed flow [Panov et al., 2010; Nakamura et al., 2013]. For the second (transient reconnection) and third (spontaneous formation) mechanisms, they have not been verified yet. Runov et al. [2012] reported a DF event associated with the reconnection onset. In that event, tailward flow and earthward flow are observed simultaneously by different spacecraft, whereas DF is only observed inside the earthward flow in the near-Earth region ($X_{\text{GSM}} \approx -9 R_E$). This event somehow supports the first mechanism (jet braking) but not the second one. To examine whether the transient reconnection can produce DFs, the observation of DFs associated with X line or inside ion diffusion region is necessary. We show such an event in this paper.

2. Observations

[5] The observations were made by Cluster around 13:12 UT on 18 September 2002. At that time, four spacecraft were located at $X_{\text{GSM}} \approx -17.5 R_E$, $Y_{\text{GSM}} \approx 4 R_E$, and $Z_{\text{GSM}} \approx 0$

¹Space Science Institute, School of Astronautics, Beihang University, Beijing, China.

²Swedish Institute of Space Physics, Uppsala, Sweden.

³Johns Hopkins University Applied Physics Laboratory, Laurel, Maryland, USA.

⁴Institute of Geophysics and Planetary Physics, University of California, Los Angeles, California, USA.

⁵School of Earth and Space Sciences, Peking University, Beijing, China.

⁶Department of Physics, Umeå University, Umeå, SE, Sweden.

⁷Laboratoire de Physique des Plasmas, Ecole Polytechnique, UPMC, Université Paris Sud, CNRS, Palaiseau, France.

⁸State Key Laboratory for Space Weather, CSSAR, Beijing, China.

⁹School of Electronic and Information, Wuhan University, Wuhan, China.

Corresponding author: H. S. Fu, Space Science Institute, School of Astronautics, Beihang University, 37 Xueyuan Rd., Haidian District Beijing, 100191 China. (huishanf@gmail.com)

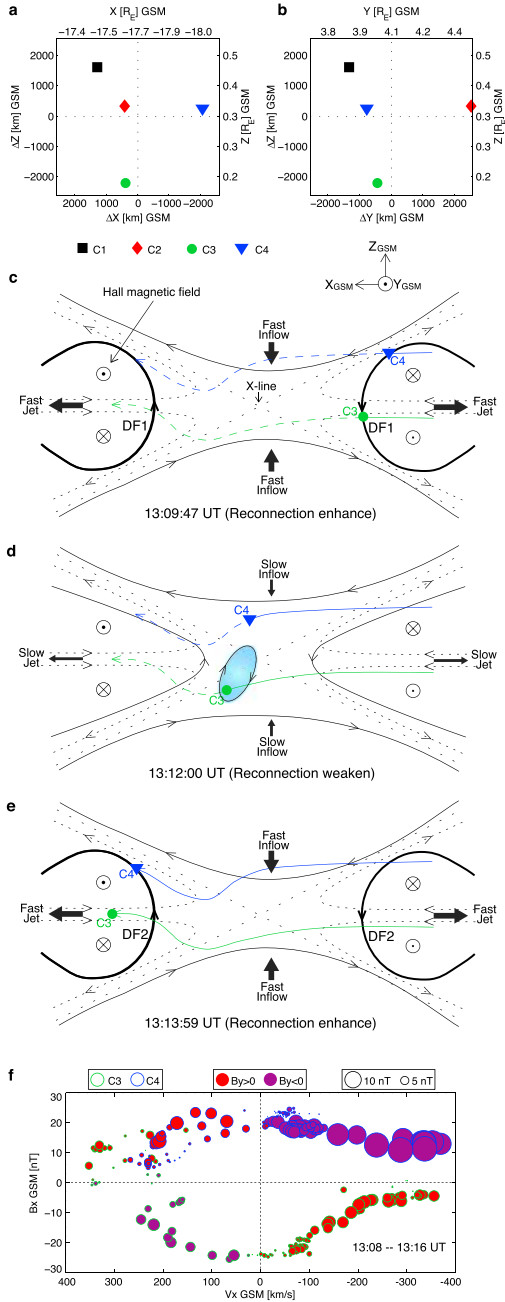


Figure 1. Cluster tetrahedron location at 13:12 UT on 18 September 2002 in (a) the X - Z plane and (b) the Y - Z plane. Separations of the four Cluster spacecraft, noted as ΔX , ΔY , and ΔZ , are also shown in the top. (c–e) Diagrams showing the evolution of ion diffusion region from 13:08 to 13:16 UT. The color lines indicate the trajectories of C3 (green) and C4 (blue), with the solid parts represent spacecraft’s history and the dashed parts represent the locations where spacecraft will arrive. DF pair is formed in Figures 1c and 1e, associated with the enhancement of reconnection rate. Color-coded circle in Figure 1d shows a magnetic island measured by C3 at 13:12 UT (during the weakening of reconnection). (f) Out of plane magnetic field B_y as a function of B_x and V_x . Red corresponds to $B_y > 0$, and purple corresponds to $B_y < 0$. The size of the circle corresponds to the magnitude of B_y , and the color of the circle corresponds to the measurements of C3 (green circle) and C4 (blue circle). Spin-resolution data and GSM coordinates are used in Figure 1.

in GSM coordinates (Figures 1a and 1b); their separation was about 3000 km. C3 and C4 captured a reconnection event from 13:08 UT to 13:16 UT (Figure 2). We illustrate this event using the cartoon in Figures 1c–1e. During the whole period, the $B_{x\text{GSM}}$ measured by C3 (green) was approximately negative (Figure 2b), while the $B_{x\text{GSM}}$ measured by C4 (blue) was positive (Figure 2b). This means that C3 and C4 passed, respectively, the southern and northern part of the current sheet (see the Cluster trajectory in Figures 1c–1e). Since the $B_{x\text{GSM}}$ measured by C3 was very small before 13:10 UT and after 13:14 UT, C3 should locate near the current sheet center at the initial and final stage of this passing. Around 13:13 UT, C4 measured small $B_{x\text{GSM}}$ components (Figure 2b), because the current sheet was flapping at that time (see the concave part of the Cluster trajectory in Figures 1c–1e). We do minimum variance analysis for this flapping current sheet (13:13:22–13:14:12 UT) and find that the maximum variance, indicating the main magnetic field reversal [Eastwood *et al.*, 2009], is along $L = (0.99, 0.13, -0.01)$ in GSM coordinates; the minimum variance, indicating the normal to the current sheet plane, is along $N = (0.00, 0.03, 1.00)$ in GSM coordinates; and the medium variance is along $M = (-0.13, 0.99, -0.03)$ in GSM coordinates. Since the main magnetic field reversal is along X_{GSM} , and the normal to the current sheet is along Z_{GSM} , we conclude that GSM coordinates used in this event are appropriate. We examine the flow velocity in this event and find that the dominant component is along X_{GSM} but not Y_{GSM} or Z_{GSM} (not shown), supporting our use of GSM coordinates as well.

[6] The C3 measurements during this period can be divided into two parts: (1) Before 13:12:00 UT, the flow velocity $V_{x\text{GSM}}$ (Figure 2d) and the magnetic field $B_{z\text{GSM}}$ (Figure 2a) were generally negative, while the $B_{y\text{GSM}}$ (Figure 2c) was positive; (2) after 13:12:00 UT, the $V_{x\text{GSM}}$ and $B_{z\text{GSM}}$ were positive, while the $B_{y\text{GSM}}$ was roughly negative. The C4 measurements had a similar trend as C3 except that the transition of $V_{x\text{GSM}}$ ($B_{z\text{GSM}}$, $B_{y\text{GSM}}$) from negative to positive was found at 13:11:30 UT. During the whole interval (13:08–13:16 UT), the statistical relations among $V_{x\text{GSM}}$, $B_{x\text{GSM}}$, and $B_{y\text{GSM}}$ (see Figure 1f) satisfy the typical feature of quadrupole structure [Eastwood *et al.*, 2009; 2010], meaning that C3 and C4 possibly captured a reconnection event. Here $B_{y\text{GSM}}$ should correspond to the Hall magnetic field inside the ion diffusion region. It switched from positive to negative in C3 measurements, but from negative to positive in C4 measurements, because the two spacecraft were located in the southern (C3) and northern (C4) part of the current sheet, respectively. In fact, this event has been identified by Eastwood *et al.* [2010] as a reconnection event without guide field.

[7] In this event, C1 did not capture the reconnection signature because it was far away from the current sheet (large Z_{GSM} , see Figures 1a and 1b). C2 was near the current sheet center; however, it had a large separation from C3 and C4 in Y_{GSM} direction. C2 did not capture the reconnection signature either, probably because the ion diffusion region was smaller than 3000 km in Y_{GSM} direction (Figure 1b).

[8] Interesting finding in this event is that there were two jumps of magnetic field $B_{z\text{GSM}}$ in the ion diffusion region (Figure 2a). One was embedded inside the tailward flow ($V_{x\text{GSM}} < 0$, see the left vertical line), while the other was inside the Earthward flow ($V_{x\text{GSM}} > 0$, see the right vertical line). We identify these two jumps as DFs as they satisfy

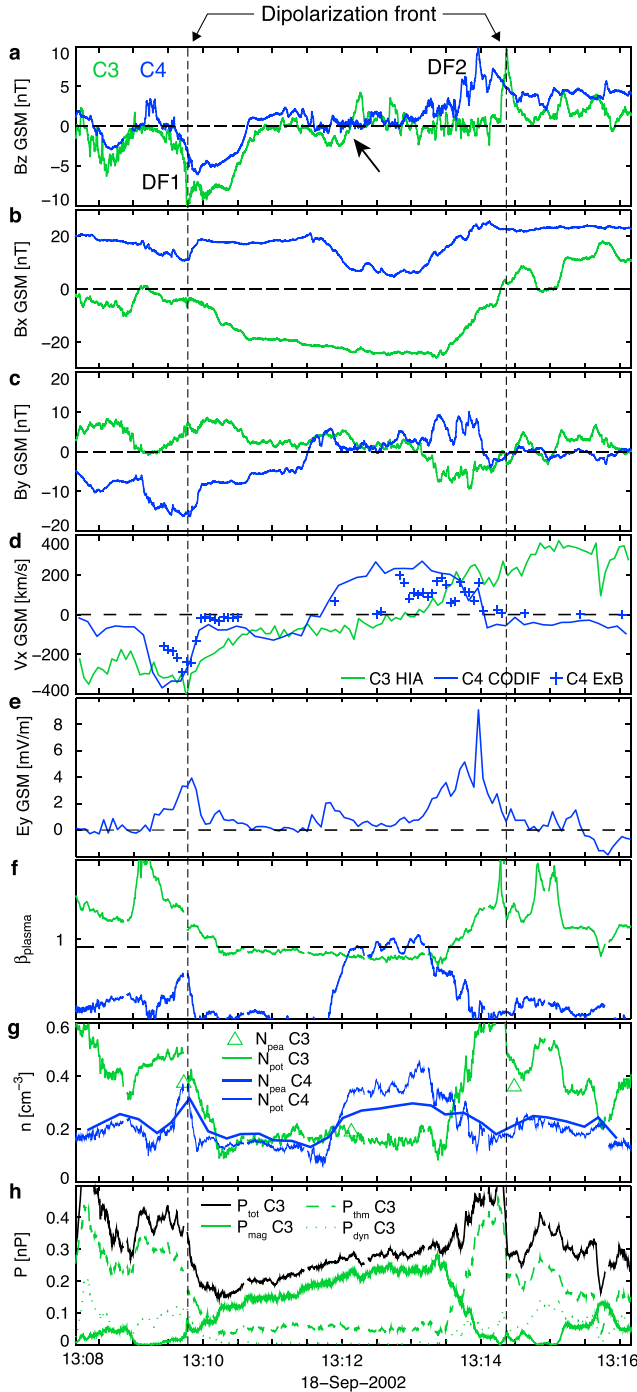


Figure 2. Cluster observations of DFs inside reconnection diffusion region. (a–c) The Z , X , Y components of magnetic field from FGM. (d) The X component of flow velocity from CIS and $\mathbf{E} \times \mathbf{B}$. (e) The Y component of electric field from EFW. (f) Plasma beta. (g) The plasma density from spacecraft potential (thin line) and from PEACE (thick line and triangles). (h) The total, thermal, magnetic, and dynamic pressures of plasmas. Data from C3 and C4 are shown in green and blue, respectively. In Figure 2e, only the data from C4-EFW are shown, because the data from C3-EFW are not reliable. In Figure 2g, the density data from C3-PEACE (triangles) have very low resolution, because parts of the data delivery time from spacecraft to ground were allocated to C3-CIS. C1 and C2 did not capture the reconnection signature in this event, so their measurements are not shown. GSM coordinates are used in Figure 2.

the following criteria [see *Runov et al., 2009; Schmid et al., 2011; Fu et al., 2012b*]: (1) $B_{z\text{GSM}}$ was the dominant component of magnetic field; (2) $B_{z\text{GSM}}$ increased/decreased more than 4 nT during several seconds, and simultaneously, the inclination angle of magnetic field increased more than 10° ; (3) the maximum inclination angle of magnetic field was larger than 45° ; (4) the maximum flow velocity, $|V_i|$, was larger than 150 km/s; (5) the plasma beta, ratio of thermal pressure to magnetic pressure, was greater than 0.5 (Figure 2f, see the horizontal dashed line). These DF structures are quite different from magnetic islands (flux ropes or plasmoids) and traveling compression regions (TCR) because the bipolar structure in $B_{z\text{GSM}}$ is not clear [see *Imber et al., 2011*]. For the magnetic island and TCR, the negative and positive $B_{z\text{GSM}}$ should have comparable amplitudes [see *Sitnov et al., 2009*]. Because C4 passed the margin of the DF structure, its observation does not strictly satisfy the definition of DF.

[9] Figure 2g shows the plasma density during the whole interval. Both the density from the PEACE instrument (N_{pea}) and the density from the spacecraft potential (N_{pot}) are plotted. The density from C3-PEACE (triangle) has very low resolution during this period, because parts of the data delivery time from spacecraft to ground were allocated to C3-CIS. There is general consistency between N_{pot} and N_{pea} , meaning that these densities are reliable. Figure 2h shows the thermal (P_{thm}), magnetic (P_{mag}), dynamic (P_{dyn}), and total (P_{tot}) pressure measured by C3. At the $B_{z\text{GSM}}$ jumps (see the vertical dashed lines), the density and thermal pressure decreased, while the magnetic pressure increased slightly. These are also typical features of DFs [see *Runov et al., 2009*]. Note that, at the DF, the total pressure (P_{tot}) is not necessary to be balanced (see discussions by *Fu et al. [2012c]*).

[10] Now we analyze in detail how spacecraft encounter the DF structures and how the ion diffusion region evolves during this period. We find that C3 and C4, separated widely in X_{GSM} direction (Figure 1a), measured the first DF (left vertical line in Figure 2) simultaneously. This phenomenon can be explained by using the cartoon in Figure 1c: C3, located at large X_{GSM} coordinates, touched the center of the DF, while C4, located at small X_{GSM} coordinates, touched the north edge of the DF. The second DF (right vertical line in Figure 2) was measured first by C4 then by C3. This DF cannot be produced simultaneously as the first one. If the two DFs are produced simultaneously and the reconnection X line moves tailward rapidly [see *Oka et al., 2011*], C3 should measure DF2 earlier than C4, as C3 had larger X_{GSM} coordinates. We describe the whole observation as follows: Cluster first measured a tailward DF, which is produced by an enhancing reconnection (Figure 1c), then slowly moved to the earthward jet and measured an earthward DF, which is produced by another enhancing reconnection (Figure 1e). From the first reconnection enhancement (13:09:47 UT, Figure 1c) to the second reconnection enhancement (13:13:59 UT, Figure 1e), the reconnection process never stops as the quadrupole structure of magnetic field is always satisfied in this event (see Figure 1f); only the reconnection rate changes. Clearly, this is an unsteady reconnection event. The change of reconnection rate is also reflected in the E_y measured by C4 (Figure 2e), although this spacecraft was not in the center of the current sheet. The spacecraft C3, located close to the current sheet center, unfortunately has no reliable measurements of electric field because one of the probes was broken.

[11] Both the time-varying inflow speed and the secondary island near the X line are possible candidates for triggering the unsteady reconnection (see discussions by *Fu et al.* [2013]). In this event, the secondary island was indeed observed by C3 at 13:12:00 UT near the X line (Figure 1d). The time-varying inflow speed, however, cannot be verified in this event, because none of the spacecraft monitor the inflow region continuously (Note that only around 13:12:00 UT was C4 located in the inflow region).

[12] In full particle simulation, *Sitnov and Swisdak* [2011] found that DFs could be formed as a consequence of transient reconnection, which is driven by a finite convection electric field outside the current sheet. In this event, Cluster observed DFs inside the ion diffusion region, strongly supporting the simulation results. The detail analysis of this event reveals that the reconnection is unsteady (transient) type, consistent with the simulation as well [*Sitnov and Swisdak*, 2011]. The secondary island suggested by *Sitnov and Swisdak* [2011] is also found in this event (see the black arrow in Figure 2a).

3. Conclusions and Discussions

[13] Up to present, there have been a lot of substructures observed inside ion diffusion region such as magnetic islands [*Huang et al.*, 2012], electron holes [*Cattell et al.*, 2005], and density cavities [*Vaivads et al.*, 2004]. Observation of dipolarization fronts inside ion diffusion region, to our knowledge, is the first time. This observation strongly supports previous simulation results [*Sitnov and Swisdak*, 2011] that transient reconnection can produce DFs.

[14] The DFs formed inside ion diffusion region are quite different from those in the near-Earth region because, in the ion diffusion region, jet braking does not happen. In fact, some studies even suggest that ions/jets are accelerated inside the diffusion region due to the bipolar electric field structure directed normal to the current sheet toward the midplane of the plasma sheet [see *Wygant et al.*, 2005; *Aunai et al.*, 2011, and reference therein]. The high-speed flow [*Cao et al.*, 2006] and the sharp increase of Bz_{GSM} are two important elements for identifying DF. In the near-Earth region, high-speed flow hits the background dipolar field, and subsequently, it slows down or even rebounds [*Panov et al.*, 2010]. During this process, magnetic fluxes pile up gradually with a front (DF) propagating tailward [*Birn et al.*, 2011; *Nakamura et al.*, 2011]. The DF is attributed to the flow in this picture, meaning that there is causality between them. Inside ion diffusion region, both flow and DF are consequences of transient reconnection. They appear simultaneously but have no causality. In fact, inside ion diffusion region, the frozen-in condition is violated, so the ions (flow) and magnetic field (DF) should have no relation.

[15] A statistical observation in the magnetotail, given by *Ohtani et al.* [2004], shows that the velocity of high-speed flow almost does not change from $X_{GSM} = -30 R_E$ to $X_{GSM} = -15 R_E$, but decrease rapidly from $X_{GSM} = -10 R_E$ to $X_{GSM} = -5 R_E$ (see Figure 5a therein). On the basis of this statistic, we suggest that the DFs measured by spacecraft in the near-Earth region ($X_{GSM} > -10 R_E$) are produced by jet braking because, in this region, the obstruction of high-speed flow by preexisting plasmas is strong; On the contrary, the DFs measured in the mid- or far-tail region ($X_{GSM} < -15 R_E$) are produced by transient reconnection or spontaneous formation because, in this region, the braking of high-speed flow is

not prominent. It is difficult to distinguish the transient reconnection from the spontaneous formation, unless the spacecraft encounter an X line structure. The observational evidence of the spontaneous formation should be invoked in the future study.

[16] **Acknowledgments.** We thank the Cluster Active Archive for providing the data for this study. For the discussions about the work, we appreciate R. Nakamura and the members of team “Particle Acceleration at Plasma Jet Fronts in the Earth’s Magnetosphere” at the ISSI. This work was supported by NSFC grants 40931054, 41204131, and 973 program 2011CB811404.

[17] The Editor thanks Kyoung-Joo Hwang and an anonymous reviewer for their assistance in evaluating this paper.

References

- Artemyev, A. V., A. A. Petrukovich, R. Nakamura, and L. M. Zelenyi (2012a), Adiabatic electron heating in the magnetotail current sheet: Cluster observations and analytical models., *J. Geophys. Res.*, *117*, A06219, doi:10.1029/2012JA017513.
- Artemyev, A. V., V. N. Lutsenko, and A. A. Petrukovich (2012b), Ion resonance acceleration by dipolarization fronts: Analytic theory and spacecraft observation, *Ann. Geophys.*, *30*, 317–324, doi:10.5194/angeo-30-317-2012.
- Artemyev, A. V., S. Kasahara, A. Y. Ukhorskiy, and M. Fujimoto (2013), Acceleration of ions in the Jupiter magnetotail: Particle resonant interaction with dipolarization fronts, *Planet. Space Sci.*, *82*, 134–148, doi:10.1016/j.pss.2013.04.013.
- Aunai, N., A. Retinò, G. Belmont, R. Smets, B. Lavraud, and A. Vaivads (2011), The proton pressure tensor as a new proxy of the proton decoupling region in collisionless magnetic reconnection, *Ann. Geophys.*, *29*, 1571–1579.
- Birn, J., R. Nakamura, E. V. Panov, and M. Hesse (2011), Bursty bulk flows and dipolarization in MHD simulations of magnetotail reconnection, *J. Geophys. Res.*, *116*, A01210, doi:10.1029/2010JA016083.
- Birn, J., A. Artemyev, D. Baker, M. Echim, M. Hoshino, and L. Zelenyi (2012), Particle acceleration in the magnetotail and aurora, *Space Sci. Rev.*, *167*, doi:10.1007/s11214-012-9874-4.
- Cao, J. B., et al. (2006), Joint observations by Cluster satellites of bursty bulk flows in the magnetotail, *J. Geophys. Res.*, *111*, A04206, doi:10.1029/2005JA011322.
- Cattell, C., et al. (2005), Cluster observations of electron holes in association with magnetotail reconnection and comparison to simulations, *J. Geophys. Res.*, *110*, A01211, doi:10.1029/2004JA010519.
- Eastwood, J. P., T. D. Phan, S. D. Bale, and A. Tjulin (2009), Observations of turbulence generated by magnetic reconnection, *Phys. Rev. Lett.*, *102*, 035001, doi:10.1103/PhysRevLett.102.035001.
- Eastwood, J. P., T. D. Phan, M. Øieroset, and M. A. Shay (2010), Average properties of the magnetic reconnection ion diffusion region in the Earth’s magnetotail: The 2001–2005 Cluster observations and comparison with simulations, *J. Geophys. Res.*, *115*, A08215, doi:10.1029/2009JA014962.
- Fu, H. S., Y. V. Khotyaintsev, M. André, and A. Vaivads (2011), Fermi and betatron acceleration of suprathermal electrons behind dipolarization fronts, *Geophys. Res. Lett.*, *38*, L16104, doi:10.1029/2011GL048528.
- Fu, H. S., Y. V. Khotyaintsev, A. Vaivads, M. André, and S. Y. Huang (2012a), Electric structure of dipolarization front at sub-proton scale, *Geophys. Res. Lett.*, *39*, L06105, doi:10.1029/2012GL051274.
- Fu, H. S., Y. V. Khotyaintsev, A. Vaivads, M. André, and S. Y. Huang (2012b), Occurrence rate of earthward-propagating dipolarization fronts, *Geophys. Res. Lett.*, *39*, L10101, doi:10.1029/2012GL051784.
- Fu, H. S., Y. V. Khotyaintsev, A. Vaivads, M. André, V. A. Sergeev, S. Y. Huang, E. A. Kronberg, and P. W. Daly (2012c), Pitch angle distribution of suprathermal electrons behind dipolarization fronts: A statistical overview, *J. Geophys. Res.*, *117*, A12221, doi:10.1029/2012JA018141.
- Fu, H. S., Y. V. Khotyaintsev, A. Vaivads, A. Retinò, and M. André (2013), Energetic electron acceleration by unsteady magnetic reconnection, *Nat. Phys.*, *9*, 426–430, doi:10.1038/NPHYS2664.
- Hamrin, M., et al. (2013), The evolution of flux pileup regions in the plasma sheet: Cluster observations, *J. Geophys. Res. Space Physics*, *118*, 6279–6290, doi:10.1002/jgra.50603.
- Huang, S. Y., et al. (2012), Electron acceleration in the reconnection diffusion region: Cluster observations, *Geophys. Res. Lett.*, *39*, L11103, doi:10.1029/2012GL051946.
- Imber, S. M., J. A. Slavin, H. U. Auster, and V. Angelopoulos (2011), A THEMIS survey of flux ropes and traveling compression regions: Location of the near-Earth reconnection site during solar minimum, *J. Geophys. Res.*, *116*, A02201, doi:10.1029/2010JA016026.

- Khotyaintsev, Y. V., C. M. Cully, A. Vaivads, M. André, and C. J. Owen (2011), Plasma jet braking: Energy dissipation and nonadiabatic electrons, *Phys. Rev. Lett.*, *106*, 165001, doi:10.1103/PhysRevLett.106.165001.
- Liu, J., V. Angelopoulos, A. Runov, and X.-Z. Zhou (2013), On the current sheets surrounding dipolarizing flux bundles in the magnetotail: The case for wedgelets, *J. Geophys. Res. Space Physics*, *118*, 2000–2020, doi:10.1002/jgra.50092.
- Lu, H. Y., et al. (2013), Electric structure of dipolarization fronts associated with interchange instability in the magnetotail, *J. Geophys. Res. Space Physics*, *118*, 6019–6025, doi:10.1002/jgra.50571.
- Nakamura, R., et al. (2002), Motion of the dipolarization front during a flow burst event observed by Cluster, *Geophys. Res. Lett.*, *29*(20), 1942, doi:10.1029/2002GL015763.
- Nakamura, R., et al. (2011), Flux transport, dipolarization, and current sheet evolution during a double-onset substorm, *J. Geophys. Res.*, *116*, A00136, doi:10.1029/2010JA015865.
- Nakamura, R., et al. (2013), Flow bouncing and electron injection observed by Cluster, *J. Geophys. Res. Space Physics*, *118*, 2055–2072, doi:10.1002/jgra.50134.
- Ohtani, S., M. A. Shay, and T. Mukai (2004), Temporal structure of the fast convective flow in the plasma sheet: Comparison between observations and two-fluid simulations, *J. Geophys. Res.*, *109*, A03210, doi:10.1029/2003JA010002.
- Oka, M., T.-D. Phan, J. P. Eastwood, V. Angelopoulos, N. A. Murphy, M. Øieroset, Y. Miyashita, M. Fujimoto, J. McFadden, and D. Larson (2011), Magnetic reconnection X-line retreat associated with dipolarization of the Earth's magnetosphere, *Geophys. Res. Lett.*, *38*, L20105, doi:10.1029/2011GL049350.
- Panov, E. V., et al. (2010), Multiple overshoot and rebound of a bursty bulk flow, *Geophys. Res. Lett.*, *37*, L08103, doi:10.1029/2009GL041971.
- Pritchett, P. L. (2010), Onset of magnetic reconnection in the presence of a normal magnetic field: Realistic ion to electron mass ratio, *J. Geophys. Res.*, *115*, A10208, doi:10.1029/2010JA015371.
- Pritchett, P. L., and F. V. Coroniti (2010), A kinetic ballooning/interchange instability in the magnetotail, *J. Geophys. Res.*, *115*, A06301, doi:10.1029/2009JA014752.
- Runov, A., V. Angelopoulos, M. I. Sitnov, V. A. Sergeev, J. Bonnell, J. P. McFadden, D. Larson, K.-H. Glassmaker, and U. Auster (2009), THEMIS observations of an earthward-propagating dipolarization front, *Geophys. Res. Lett.*, *36*, L14106, doi:10.1029/2009GL038980.
- Runov, A., V. Angelopoulos, and X.-Z. Zhou (2012), Multipoint observations of dipolarization front formation by magnetotail reconnection, *J. Geophys. Res.*, *117*, A05230, doi:10.1029/2011JA017361.
- Schmid, D., M. Volwerk, R. Nakamura, W. Baumjohann, and M. Heyn (2011), A statistical and event study of magnetotail dipolarization fronts, *Ann. Geophys.*, *29*, 1537–1547, doi:10.5194/angeo-29-1537-2011.
- Sergeev, V., V. Angelopoulos, S. Apatenkov, J. Bonnell, R. Ergun, R. Nakamura, J. McFadden, D. Larson, and A. Runov (2009), Kinetic structure of the sharp injection/dipolarization front in the flow-braking region, *Geophys. Res. Lett.*, *36*, L21105, doi:10.1029/2009GL040658.
- Sitnov, M. I., and M. Swisdak (2011), Onset of collisionless magnetic reconnection in two-dimensional current sheets and formation of dipolarization fronts, *J. Geophys. Res.*, *116*, A12216, doi:10.1029/2011JA016920.
- Sitnov, M. I., M. Swisdak, and A. V. Divin (2009), Dipolarization fronts as a signature of transient reconnection in the magnetotail, *J. Geophys. Res.*, *114*, A04202, doi:10.1029/2008JA013980.
- Sitnov, M. I., N. Buzulukova, M. Swisdak, V. G. Merkin, and T. E. Moore (2013), Spontaneous formation of dipolarization fronts and reconnection onset in the magnetotail, *Geophys. Res. Lett.*, *40*, 22–27, doi:10.1029/2012GL054701.
- Vaivads, A., Y. Khotyaintsev, M. André, A. Retinò, S. C. Buchert, B. N. Rogers, P. Décreau, G. Paschmann, and T. D. Phan (2004), Structure of the magnetic reconnection diffusion region from four-spacecraft observations, *Phys. Rev. Lett.*, *93*, 105001, doi:10.1103/PhysRevLett.93.105001.
- Vaivads, A., A. Retino, Y. V. Khotyaintsev, and M. Andre (2011), Suprathermal electron acceleration during reconnection onset in the magnetotail, *Ann. Geophys.*, *29*, 1917–1925, doi:10.5194/angeo-29-1917-2011.
- Volwerk, M., et al. (2008), Magnetotail dipolarization and associated current systems observed by Cluster and Double Star, *J. Geophys. Res.*, *113*, A08S90, doi:10.1029/2007JA012729.
- Wu, M. Y., Q. M. Lu, M. Volwerk, Z. Vörös, T. L. Zhang, L. C. Shan, and C. Huang (2013), A statistical study of electron acceleration behind the dipolarization fronts in the magnetotail, *J. Geophys. Res. Space Physics*, *118*, 4804–4810, doi:10.1002/jgra.50456.
- Wygant, J. R., et al. (2005), Cluster observations of an intense normal component of the electric field at a thin reconnecting current sheet in the tail and its role in the shock-like acceleration of the ion fluid into the separatrix region, *J. Geophys. Res.*, *110*, A09206, doi:10.1029/2004JA010708.
- Zhou, M., X. H. Deng, M. Ashour-Abdalla, R. J. Walker, Y. Pang, C. Tang, S. Y. Huang, M. El-Alaoui, Z. G. Yuan, and H. M. Li (2013), Cluster observations of kinetic structure and electron acceleration within a dynamic plasma bubble, *J. Geophys. Res. Space Physics*, *118*, 674–684, doi:10.1029/2012JA018323.